Distribution of relaxation times from dielectric spectroscopy using Monte Carlo simulated annealing: Application to α-PVDF

A. Bello and E. Laredo
Department of Physics, Universidad Simón Bolívar, Apartado 89.000, Caracas 1081, Venezuela

M. Grimau
Department of Materials Science, Universidad Simón Bolívar, Apartado 89.000, Caracas 1081, Venezuela

(Received 16 December 1998; revised manuscript received 8 July 1999)

The existence of a distribution of relaxation times has been widely used to describe the relaxation function versus frequency in glass-forming liquids. Several empirical distributions have been proposed and the usual method is to fit the experimental data to a model that assumes one of these functions. Another alternative is to extract from the experimental data the discrete profile of the distribution function that best fits the experimental curve without any *a priori* assumption. To test this approach a Monte Carlo algorithm using the simulated annealing is used to best fit simulated dielectric loss data, $\varepsilon''(\omega)$, generated with Cole-Cole, Cole-Davidson, Havriliak-Negami, and Kohlrausch-Williams-Watts (KWW) functions. The relaxation times distribution, $G(\ln(\tau))$, is obtained as an histogram that follows very closely the analytical expression for the distributions that are known in these cases. Also, the temporal decay functions, $\phi(t)$, are evaluated and compared to a stretched exponential. The method is then applied to experimental data for α-polyvinylidene fluoride over a temperature range 233 K$\leqslant T\leqslant$278 K and frequencies varying from 3 MHz to 0.001 Hz. These data show the existence of two relaxation processes: the fast segmental α_a process associated with the glass transition and a α_c mode, which is slower and due to changes in conformation that can occur in the crystalline regions. The experimental curves are fitted by the simulated annealing direct signal analysis procedure, and the relaxation times distributions are calculated and found to vary with temperature. The decay function is also evaluated and it shows clearly its bimodal character and a good agreement with a KWW function with a temperature dependent β for each mode. The relaxation plots are drawn for each mode and the Vogel-Tammann-Fulcher and Arrhenius parameters are found. The fragility parameter for polyvinylidene flouride (PVDF) is found to be 87, which characterizes this polymer as a relatively structurally strong material. [S0163-1829(99)13641-5]

I. INTRODUCTION

In experimental studies on polymer dynamics with broadband dielectric spectroscopy (DS) the variation of the real, ε', and imaginary part, ε'', of the dielectric constant as a function of temperature, T, and angular frequency, ω, is obtained. Many attempts have been made to explain the broad frequency range of $\varepsilon''(\omega)$. In the case of glass-forming liquids, the experimental behavior has been described by assuming a distribution function for the relaxation times contributing to each relaxation process. The general approach, widely used to describe the experimental data, has been to assume an exponential decay function together with an empirical distribution function, $G(\ln(\tau))$, which describes the superposition of exponentially damped processes and to best fit the parameters that define this function to the experimental data.[1–3]

Several empirical functions have been used in glass-forming polymeric materials to describe the variation of $\varepsilon^*(\omega)$, such as the Cole-Cole,[4] the Davidson-Cole,[5] and the Havriliak-Negami[6] relaxation functions. From these expressions the distribution of relaxation times can be analytically found. When the parameters that characterize the width and skewness, if any, are equal to 1 all these expressions result in the Debye equation. The first one is a symmetric distribution function, while the second and third are characterized by an asymmetric profile. The Havriliak-Negami distribution function has been the most widely used not only to interpret dielectric spectroscopy[7] data but also in the case of quasi-elastic neutron-scattering data.[8] It describes the relaxation function with three adjustable parameters, τ_{HN}, the mean relaxation time value, and α and γ, which represent the width and skewness of the dielectric loss when represented as a function of $\log(\omega)$. In Table I we have summarized the expressions corresponding to the different empirical models for $\varepsilon^*(\omega)$, $\varepsilon''(\omega)$, and $G(\ln(\tau))$. On the other hand, the Kohlrausch-Williams-Watts[9] (KWW), the so-called stretched exponential:

$$\phi(t)=\exp\left[-\left(\frac{t}{\tau_{KWW}}\right)^{\beta}\right] \tag{1}$$

has been widely used and fits well the experimental data in a wide variety of experimental techniques, such as dielectric and mechanical relaxations, light scattering, and NMR. The theoretical justification for this nonexponential decay has been found either in the simplest version of Ngai's[10] coupling model or in the most recent version of the model,[11] which adds an inhomogeneous distribution of primitive relaxation times.

An alternative to the approaches briefly listed above is a direct numerical determination of the distribution function, $G(\ln(\tau))$, from the experimental data $\varepsilon^*(\omega)$, which with the

TABLE I. Analytical expressions of $\varepsilon^*(\omega)$, $\varepsilon''(\omega)$, and $G(\ln\tau)$ for the theoretical models most used for the complex dielectric constant ($\varepsilon^* = \varepsilon' - i\varepsilon''$ and $\Delta\varepsilon = \varepsilon_0 - \varepsilon_\infty$).

Model	$\varepsilon^*(\omega) - \varepsilon_\infty$	$\varepsilon''(\omega)$	$G(\ln(\tau))$
Debye	$\dfrac{\Delta\varepsilon}{1+i\omega\tau_0}$	$\dfrac{\Delta\varepsilon\ \ \omega\tau_0}{1+(\omega\tau_0)^2}$	———
Cole-Cole	$\dfrac{\Delta\varepsilon}{1+(i\omega\tau_0)^\alpha}$	$\dfrac{\Delta\varepsilon(\omega\tau_0)^\alpha \sin(\pi\alpha/2)}{1+2(\omega\tau_0)^\alpha\cos(\pi\alpha/2)+(\omega\tau_0)^{2\alpha}}$	$\dfrac{1}{2\pi}\left(\dfrac{\sin(\pi\alpha)}{\cosh(\alpha\ln(\tau/\tau_0))+\cos(\pi\alpha)}\right)$
Davidson-Cole	$\dfrac{\Delta\varepsilon}{(1+i\omega\tau_0)^\gamma}$	$\Delta\varepsilon(\cos(\varphi))^\gamma\sin(\gamma\varphi)$ with $\varphi=\tan^{-1}(\omega\tau_0)$	$\begin{cases}\dfrac{\sin(\gamma\pi)}{\pi}\left(\dfrac{\tau}{\tau_0-\tau}\right)^\gamma, & \tau<\tau_0\\ 0, & \tau>\tau_0\end{cases}$
Havriliak-Negami	$\dfrac{\Delta\varepsilon}{(1+(i\omega\tau_0)^\alpha)^\gamma}$	$\dfrac{\Delta\varepsilon\sin(\gamma\varphi)}{(1+2(\omega\tau_0)^\alpha\cos(\pi\alpha/2)+(\omega\tau_0)^{2\alpha})^{\gamma/2}}$ with $\varphi=\tan^{-1}\left(\dfrac{(\omega\tau_0)^\alpha\sin(\pi\alpha/2)}{1+(\omega\tau_0)^\alpha\cos(\pi\alpha/2)}\right)$	$\dfrac{(\sin(\gamma\theta))/\pi}{(1+2(\tau/\tau_0)^\alpha\cos(\pi\alpha/2)+(\tau/\tau_0)^{2\alpha})^{\gamma/2}}$ with $\theta=\dfrac{\pi}{2}-\tan^{-1}\left(\dfrac{(\tau_0/\tau)^\alpha+\cos(\pi\alpha)}{\sin(\pi\alpha)}\right)$
Kohlrausch-Williams-Watts	$\Delta\varepsilon\displaystyle\int_0^\infty\left[-\frac{d\phi(t)}{dt}\right]e^{-i\omega t}dt$ with $\phi(t)=\exp(-(t/\tau_0)^\beta)$	$\Delta\varepsilon\displaystyle\int_0^\infty e^{-x}\sin(\omega\tau_0 x^{1/\beta})dx$	$\dfrac{1}{\pi}\displaystyle\int_0^\infty e^{-x}e^{-u\cos(\pi\beta)}\sin[u\sin(\pi\beta)]dx$ with $u=\left(\dfrac{x\tau}{\tau_0}\right)^\beta$ $\left(\dfrac{\tau}{4\pi\tau_0}\right)^{\frac{1}{2}}e^{-\pi/4\tau_0}$, for $\beta=\frac{1}{2}$

new advances in dielectric instrumentation can be measured in a broad frequency band. The first attempt in this direction was made by Imanishi *et al.*,[12] who calculated the relaxation spectrum $G(\ln(\tau))$ by using the histogram method; it consists of fitting the experimental curve with an histogram of relaxation times, the height of each bar being the contribution of the mode with that τ to the whole relaxation spectrum. The method was applied to the analysis of the master curves obtained for bulk and concentrated solutions of *cis*-polyisoprene for both the segmental and the normal modes. The CONTIN procedure of Provencher[13] was then applied to the dielectric data of poly(hydroxy ether of bisphenol-A) by Alvarez *et al.*[7] and Karatasos *et al.*[14] in the case of the dielectric normal mode in diblock polymers. Recently, Schäfer *et al.*[15] have proposed a different method to extract the continuous distribution of relaxation times from the complex dielectric spectra by solving a Fredholm integral equation using the Tikhonov regularization technique with self-consistent choice of the regularization parameter. They applied the procedure to simulated curves using two or four slightly Gaussian broadened overlapping processes, and found an acceptable agreement between the extracted $G(\ln(\tau))$ and that used in the simulation of the complex spectrum. Experimental curves obtained with salol adsorbed on microporous glass were also fitted with this procedure and interesting results were obtained for $G(\ln(\tau))$ as a function of temperature.

In this paper we present an approach for extracting the distribution of relaxation times from the broad-band dielectric spectra of glass-forming materials by using the simulated annealing Monte Carlo procedure[16] together with the direct signal analysis[17] in order to decompose the relaxation spectrum into true Debye components, which contribute to the spectrum according to the relaxation times distribution. To check the validity of the procedure it is first applied to computer generated $\varepsilon''(\omega)$ curves based on known distribution profiles whose analytical expressions are known (see Table I). Then, the method is applied to find the temperature variation of the relaxation times distribution for α-polyvinylidene flouride (α-PVDF) (Ref. 18) obtained over a wide frequencies range. It is shown that the computer procedure proposed here is able to capture the fine details of $G(\ln(\tau))$ that best fit the experimental data. Previous results on α or β polymorph of PVDF were made by DS on the somewhat restricted frequency range that was available at that time[19,20] and showed the presence of two relaxation modes; the α_a mode, which is related to the glass transition occurring in the amorphous zones and the α_c that is originated in the crystalline zones of the polymer. The quantitative results on the relaxation times involved in the α_c relaxation reported in these previous works, differ from the more recent determinations made by two-dimensional (2D) exchange deuteron NMR by Hirschinger *et al.*[21] More recent determinations of the relaxation plots on β-PVDF and the effect of high pressure have been made by Samara[22] for the α_a mode. The variation of both the α_c and α_a modes with frequency and temperature are reported here in a broader frequency range, and the simulated annealing direct signal analysis (SADSA) procedure is applied to extract $G(\ln(\tau))$ at

each temperature together with the decay function $\phi(t)$ and the relaxation plots for this important material.

II. EXPERIMENT

A. Materials

The polyvinylidene fluoride (PVDF) used in this work was from Solvay Cie. (SolefX8N). Its structure corresponds to the nonferroelectric, nonpiezoelectric α-crystalline form of this polymer. Films were compression molded from pellets at 503 K and 5000 psi. Their average thickness is 150 μm. After molding, the samples were slowly cooled to room temperature and gold electrodes were sputtered to improve the contacts with the gold-plated electrodes of the cell. The degree of crystallinity, X_c, is determined from the area of the melting peak obtained by differential scanning calorimetry in a Perkin-Elmer DSC-7 and found to be 50%; this value is calculated using 6.7 kJ/mole as the heat of fusion for a 100% crystalline PVDF.

B. Broad-band dielectric spectroscopy

The broad-band dielectric-spectrometer is a Concept Twelve from Novocontrol for $f \leqslant 3\times10^6$ Hz. The sample resides between two gold-plated electrodes 30 mm in diameter in a cryostat in a cold nitrogen-gas stream. The measurements of the real, ε', and imaginary part, ε'', of the dielectric constant as a function of angular frequency, ω, are obtained at each temperature, T, by using a Solartron S1-1260 impedance analyzer and a Quatro temperature controller. The 37 frequencies range from 10^{-3} to 3×10^6 Hz and the temperatures used here go from 223 K to 313 K in 2.5 K steps. The temperature stabilization is better than 0.1 K and the resolution in tan δ better than 10^{-4}. For higher frequencies an HP4291A RF impedance analyzer is used in a coaxial line reflectometry setup for $1\times10^6\text{Hz} \leqslant f \leqslant 1.8\times10^9\text{Hz}$.

III. THEORETICAL BACKGROUND

The frequency-dependent complex dielectric constant defined as:

$$\varepsilon^* = \varepsilon' - i\varepsilon'', \tag{2}$$

has the following expression for a Debye process:

$$\varepsilon^* = \varepsilon_\infty + \frac{\varepsilon_0 - \varepsilon_\infty}{1 + i\omega\tau}, \tag{3}$$

where τ is a single-valued, temperature-dependent, relaxation time following an Arrhenius or a Vogel-Tammann-Fulcher (VTF) expression:

$$\tau(T) = \tau_0 \exp\left[\frac{E}{kT}\right], \quad \tau_{VTF}(T) = \tau_{0_{VTF}} \exp\left[\frac{E_{VTF}}{k(T - T_0)}\right]. \tag{4}$$

If we assume that the relaxation function is made by the superposition of M independent Debye-like processes with a continuous normalized distribution of relaxation times $G(\ln(\tau))$ then

$$\varepsilon^*(\omega, T) = \varepsilon_\infty + \Delta\varepsilon \int_{-\infty}^{+\infty} \frac{G(\ln(\tau))}{1 + i\omega\tau} d\ln(\tau), \tag{5}$$

with $\Delta\varepsilon = \varepsilon_0 - \varepsilon_\infty$ and the normalization condition

$$\int_{-\infty}^{\infty} G(\ln(\tau)) d\ln(\tau) = 1. \tag{6}$$

Then the real and imaginary part of the complex permittivity are given by:

$$\varepsilon'(\omega, T) = \varepsilon_\infty + \Delta\varepsilon \int_{-\infty}^{+\infty} \frac{G(\ln(\tau))}{1 + \omega^2\tau^2} d\ln(\tau), \tag{7}$$

$$\varepsilon''(\omega, T) = \Delta\varepsilon \int_{-\infty}^{+\infty} \frac{G(\ln(\tau))\omega\tau}{1 + \omega^2\tau^2} d\ln(\tau). \tag{8}$$

From these expressions it appears that the distribution function can be calculated numerically from the dielectric data. In the next section the SADSA algorithm used to perform this task is explained in detail.

Now, if one wants to switch to the time domain, the decay function $\phi(t)$ can also be calculated by a numerical integration if the distribution of relaxation times is known:

$$\phi(t) = \int_{-\infty}^{+\infty} G(\ln(\tau)) \exp\left[-\left(\frac{t}{\tau}\right)\right] d\ln(\tau). \tag{9}$$

At this point, when $\phi(t)$ is obtained it can be fitted to a KWW decay function and the τ_{KWW} and β parameters fitted.

IV. DATA ANALYSIS

The distribution of relaxation times can be found from Eq. (5) if the complex dielectric constant is known, by solving this integral equation for $G(\ln(\tau))$. Several methods are available to perform this operation. If an expression for $\varepsilon^*(\omega)$ is known in closed form, it is possible to calculate an analytical expression of $G(\ln(\tau))$ by means of the inverse Stieltjes transform[5,23] as follows:

$$G(\ln(\tau)) = \frac{1}{2\pi i}\left[\varepsilon^*\left(\frac{e^{-i\pi}}{\tau}\right) - \varepsilon^*\left(\frac{e^{i\pi}}{\tau}\right)\right]. \tag{10}$$

Equation (10) has been applied to the most common empirical equations of $\varepsilon^*(\omega)$ and the results are shown in the fourth column of Table I. It is worth mentioning that the result shown here for the Havriliak-Negami distribution function somewhat differs from expressions previously published. For example, Böttcher and Bordewijk[23] and more recently Havriliak and Havriliak[24] both show expressions that can lead to negative values of $G(\ln(\tau))$ for a certain combination of the Havriliak-Negami parameters. This can be seen from the expression given for the angle Θ by Havriliak and Havriliak[24] [their Eq. (3)], where for values of $\alpha > 0.5$ there will always be a range of τ/τ_0 for which $\Theta < 0$. Upon substituting this negative Θ value in the expression for the distribution function [their Eq. (2)] a negative value for $G(\ln(\tau))$ results. The problem is not solved by taking the absolute value of Θ as suggested by Alvarez *et al.*[7] as the obtained distribution profile is still not correct. Instead, by taking the complement of Θ as indicated in Table I the distribution is positive for all combinations of parameters over

the whole τ range. This modification has already been noted by Bertelsen and Lindgård[25] and by Schönhals.[26]

As one of the objectives for obtaining $G(\ln(\tau))$ is to deduce the decay correlation function, $\phi(t)$, with Eq. (9) in order to switch to the time domain, this can be done by fitting the experimental $\varepsilon''(\omega)$ data to the Havriliak-Negami expression and then using the α and γ parameters obtained to evaluate $G(\ln(\tau))$ with the theoretical expression given in Table I. Nevertheless, this method is based on the assumption that the distribution of relaxation times is indeed Havriliak-Negami, and it is also very difficult to apply when the experimental curves are made of overlapping modes.

When dealing with experimental data for $\varepsilon^*(\omega)$, it is necessary to use numerical methods in order to obtain $G(\ln(\tau))$. One way is the use of the inverse Fourier transform of Eq. (8) as suggested by Franklin and de Bruin[27] and later improved by Liedermann and Loidl.[28] This method has the usual problems of discrete Fourier transforms: truncation, aliasing and computing rounding error effects, noisy data, and the need of the data points to be available at frequencies located at equidistant short intervals on a logarithmic scale. Another approach is the use of the CONTIN program of Provencher[13] as suggested by Alvarez *et al.*[7] and Karatasos *et al.*[14] More recently, Schäfer *et al.* [15] have extracted the continuous distribution of relaxation times from complex dielectric spectra using the Tikhonov regularization technique with the self-consistency method of Honerkamp and Weese.[29,30] Finally, Eq. (8) can be inverted by discretizing the distribution function into a sum of M contributions or bins, each characterized by a pair (τ_k, G_k). The dielectric loss can then be written as:

$$\varepsilon''(\omega) = \sum_{k=1}^{M} \frac{G_k \omega \tau_k}{1+\omega^2 \tau_k^2}. \tag{11}$$

Colonomos and Gordon[31] used this concept along with the Simplex method of optimization for analyzing experimental dielectric data from isoamyl bromide. Imanishi et al.[12] with the histogram method, find the distribution of relaxation times by discretizing it and using an iterative method in order to minimize the differences between the observed and calculated values of $\varepsilon''(f_i)$ where f_i are the measurement frequencies and choosing the discrete relaxation times as $\tau_i = 1/2\pi f_i$.

In this work we propose the use of the simulated annealing direct signal analysis (SADSA) method,[32] which has been successfully used in the analysis of relaxation curves from thermally stimulated depolarization current experiments. The algorithm has been properly modified for the analysis of experimental dielectric loss curves as a function of frequency. Each relaxation peak is decomposed into M elementary modes, i.e., Debye relaxation processes, which contributes to the whole spectrum an amount G_k; then, all the contributions are summed as expressed in Eq. (11). It is to be noted that the procedure is applicable if the relaxation mode can be decomposed in a sum of Debye processes. The applicability of such a forced-fitting method is in each case justified by the quality of the results, but the initial assumption might not be true in some cases. The method is somewhat similar to the histogram method of Imanishi, but instead, here the sum of the square residuals among the observed and calculated ε'' is minimized to optimize the expression:

$$\chi^2 = \sum_{i=1}^{N} [\varepsilon''_{\text{obs}}(\omega_i) - \varepsilon''_{\text{cal}}(\omega_i)]^2, \tag{12}$$

where ω_i are the experimental angular frequencies and N is the number of data points. This optimization could be done using standard linear least squares methods such as singular value decomposition,[33] since the problem is linear in the G_k parameters; this method does not guarantee that all the G_k will be positive as required. Another approach is to use nonlinear least squares (Marquardt-Levenberg) (Ref. 33), constraining the parameters to be positive. This method is highly sensitive to the choice of initial parameters and there is not a guarantee that the minimum reached would be the global one that is sought. Usually one obtains a local minimum and several runs must be made with different initial parameters to ensure that the best fit has been reached. To avoid these problems, we use the simulated annealing optimization method of Kirkpatrick *et al.*[16] appropriately modified to handle continuous functions, to optimize Eq. (12). Even though this algorithm is now well known and widely used in all kinds of optimization problems,[33] we will briefly describe it and explain the particulars of its application in this work.

At the heart of the SADSA method is the so-called Metropolis criterion:[34] a simulated thermodynamic system is assumed to change its configuration from energy E_1 to energy E_2 with probability $p = \exp[(E_2 - E_1)/T]$. If $E_2 < E_1$ the probability is arbitrarily assigned a value $p = 1$, so downhill steps are always taken. But if $E_2 > E_1$ then an uphill step is taken sometimes depending on the temperature. In the SADSA, the function to be minimized is the value of χ^2 from Eq. (12) and the ''temperature'' is a control parameter with the same units as χ^2. At any given ''temperature'' the values of the parameters being adjusted are changed by randomly exploring the parameters space and χ^2 is calculated anew; the new values are accepted or rejected according to the Metropolis criterion. Each of these trials is called a Monte Carlo step and a large number of these are performed until the mean value of χ^2 reaches a stable value or a predetermined limiting number of steps is done. The variation of the parameters is controlled via an adaptive factor recalculated every N_s Monte Carlo steps in a way that at every ''temperature'' the number of accepted steps is roughly equal to the number of rejected steps following the recipe of Corana *et al.*[35] We start at some ''high temperature'' and after ''thermal equilibration'' the ''temperature'' is lowered, usually by a factor between 0.95 and 0.99, and the Monte Carlo steps are repeated at the new ''temperature.'' This annealing schedule corresponds to what is called in the literature the fast simulated annealing.[36] The process is stopped at a ''temperature'' low enough where no more significant improvements can be expected for the χ^2 value.

The number of parameters to be fitted, M, that is, the number of bins of the histogram is in principle arbitrary. One normally chooses the minimum necessary to approach satisfactorily the distribution function. More important is the choice of the range of τ_k. It must be sufficiently broad to cover all the relaxation times that will contribute to the ex-

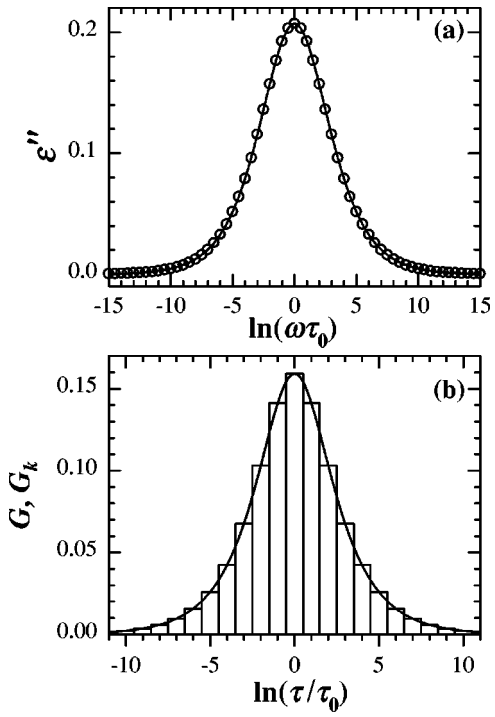

FIG. 1. SADSA results for a computer generated $\varepsilon''(\omega)$ with a Cole-Cole function ($\alpha=0.5$): (a) ($\bigcirc$) generated points, —— fitted curve; (b) G_k histogram, $G(\ln(\tau))$—— from analytical expression.

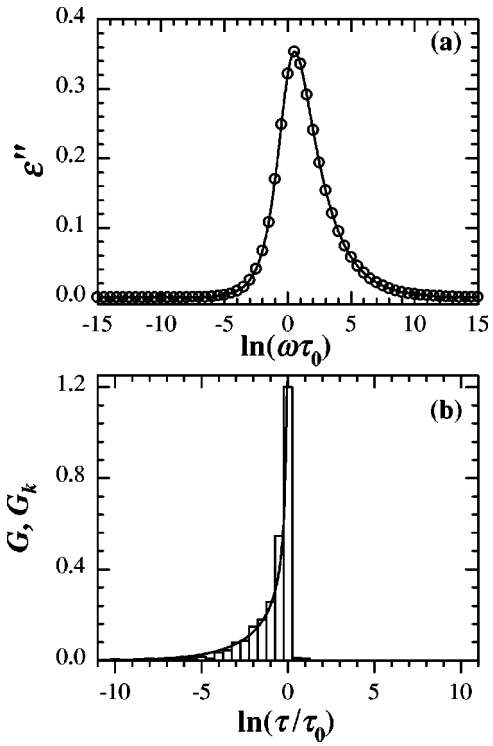

FIG. 2. SADSA results for a computer generated $\varepsilon''(\omega)$ with a Davidson-Cole function ($\gamma=0.5$): (a) ($\bigcirc$) generated points, —— fitted curve; (b) G_k histogram, $G(\ln(\tau))$ —— from analytical expression.

perimental relaxation curve but not too narrow to minimize edge effects, that is, the extreme bins contributing in excess of what they should. Usually after two or three runs of the program, one gets a clear idea of the appropriate range and number of bins necessary for a successful fitting. These preliminary fittings are usually done lowering the ''temperature'' using a reduction factor of 0.9. In the definitive runs, the factor is usually 0.975, which lowers the ''temperature'' slower than before. The set of τ_k are selected equally spaced in logarithm space, that is, a constant $\Delta(\ln(\tau_k))=\ln(\tau_{k+1})-\ln(\tau_k)$, and in practice we found that $\Delta(\ln(\tau_k))=1$ was sufficient to extract the distribution function in most cases. The initial values of the G_k were all the same, i.e., a box-shaped distribution, and the discrete initial distribution is normalized, i.e., $G_k=1/M$, $\forall k$. Finally the initial ''temperature'' is usually taken as $100\chi_0^2$, where χ_0^2 is the initial value of the sum of square residuals. The program was carefully validated using computer-generated curves as will be explained in the next section.

V. RESULTS AND DISCUSSION

A. Computer-generated curves

The proposed method for determination of $G(\ln(\tau))$ was first investigated using computer-generated curves for ε'' for the models listed in Table I. All the curves were generated with $\Delta\varepsilon=1$ and the characteristic relaxation time $\tau_0=1$ s. For the Cole-Cole distribution function the shape parameter is taken as: $\alpha=0.5$ and an $\omega\tau_0$ range corresponding to $-30\leqslant\ln(\omega\tau_0)\leqslant 30$. The $\varepsilon''(\omega)$ curve is fitted with the SADSA procedure and in Fig. 1(a) the generated curve (open circles) together with the best fit (continuous curve) are represented. The agreement is excellent and it is quantified by the sum of square residuals $\chi^2=9.4\times10^{-9}$. In Fig. 1(b) the resulting relaxation-time distribution function is plotted as a histogram, the height of each bar representing the contribution of this particular Debye process to the complex curve. If, now, $G(\ln(\tau))$ is analytically calculated from the expression given in the third row of the last column of Table I, the continuous curve in Fig. 1(b) is obtained. The agreement found between the numerically discretized distribution function and the analytical one ensures the validity of our procedure. The same calculations are carried out in the case of the Davidson-Cole distribution function with $\gamma=0.5$. The results plotted on Fig. 2(a) show again a very satisfactory agreement ($\chi^2=5.0\times10^{-7}$). Also, the continuous distribution function calculated analytically is very near to the discrete one represented by the histogram in Fig. 2(b). The typical features of this distribution function are readily observed, i.e., an asymmetric relaxation function due to a steep cutoff in $G(\ln(\tau))$ for $\tau=\tau_0$.

On going to the fifth row of Table I, the widely used Havriliak-Negami[6] distribution function is found. In Fig. 3(a) the asymmetric function resulting from the computer generated $\varepsilon''(\omega)$ is represented for $\alpha=0.6$ and $\gamma=0.3$. Here again the agreement is of high quality, $\chi^2=7.7\times10^{-8}$, and the histogram is very close to the continuous curve generated with the analytical expression written in column 4, row 5 of Table I.

Finally, the KWW function is tested. The curves for $0.1<\beta<1$ are generated numerically by integrating the expression in column 3, row 6. It is worth mentioning that there are a number of approximations to this expression in the literature[9,37–39] as an alternative to brute-force numerical in-

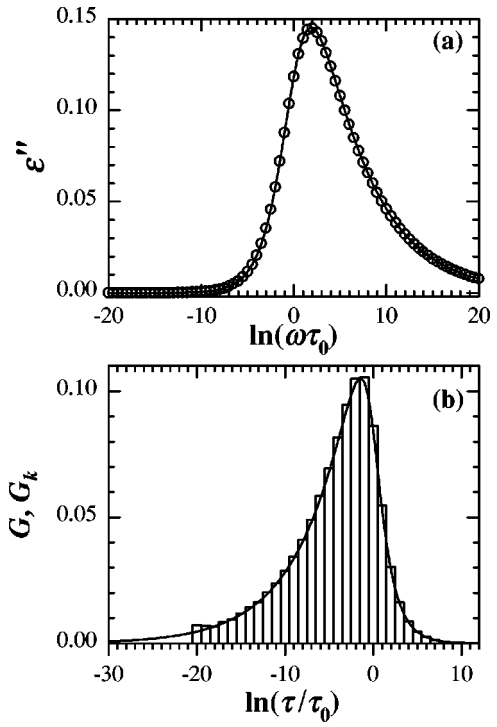

FIG. 3. SADSA results for a computer generated $\varepsilon''(\omega)$ with a Havriliak-Negami function ($\alpha=0.6$, $\gamma=0.3$): (a) ($\bigcirc$) generated points, —— fitted curve; (b) G_k histogram, $G(\ln(\tau))$ —— from analytical expression.

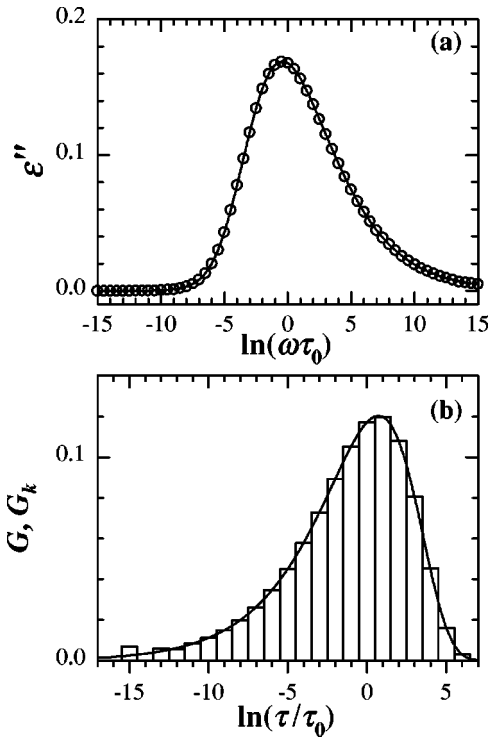

FIG. 4. SADSA results for a computer generated $\varepsilon''(\omega)$ with a KWW function ($\beta=0.3$): (a) ($\bigcirc$) generated points, —— fitted curve; (b) G_k histogram, $G(\ln(\tau))$ —— from analytical expression.

tegration. All these expressions are used and compared and the result is that the computer-generated curves do not show any significant differences with the approximations cited above. The curve generated with $\beta=0.3$ is represented in Fig. 4(a) (open symbols), the continuous curve is the result of the SADSA fitting. The asymmetry of the dielectric function is readily observed; here the quality of the fitting is again measured by the sum of square residuals which is now $\chi^2=1.4\times10^{-7}$. The discretized $G(\ln(\tau))$ obtained from the best SADSA fit is represented in Fig. 4(b) as an histogram and the continuous curve is calculated by using the analytical expression for $G(\ln(\tau))$ given in the last cell of Table I.

Once the validity of our fitting procedure has been proved the next step is to go from the frequency to the time domain by using the SADSA determined normalized distribution function, $G(\ln(\tau))$, to numerically evaluate the decay function, $\phi(t)$, by means of expression (9). In Fig. 5 the results for the numerical calculation of $\phi(t)$ are plotted as a function of $\ln(t/\tau_{KWW})$ for the four distribution functions used above. The parameter τ_{KWW} is defined as the time where the decay function reaches a value of $1/e$. The curves smoothly decay from 1 to 0, and their shape strongly depends on the parameters used for the simulation. For the three curves with a single shape parameter, i.e., Cole-Cole, Davidson-Cole, and KWW, the value of this parameter used in the simulation is 0.5 but it leads to different curve profiles. The fastest decay corresponds to the Davidson-Cole and the slowest to the Cole-Cole. The KWW decay function is intermediate. The continuous curves on this figure are the fittings of these decay functions to a KWW stretched exponential written in Eq. (1). The fitting to a KWW of the $\phi(t)$ resulting from the Cole-Cole distribution ($\beta=0.373$, $\tau_{KWW}=1.881$ s), is not satisfactory, which is to be expected as the skewness of the curve is absent in the symmetric Cole-Cole distribution. For the Davidson-Cole distribution, the best fit of $\phi(t)$ to a KWW is obtained for $\beta=0.719$, $\tau_{KWW}=0.556$ s; the difference in the shape parameters, $\beta=0.719$ and $\gamma=0.5$, shows that the KWW broadens the profiles more effectively than the Davidson-Cole with its steep cutoff.

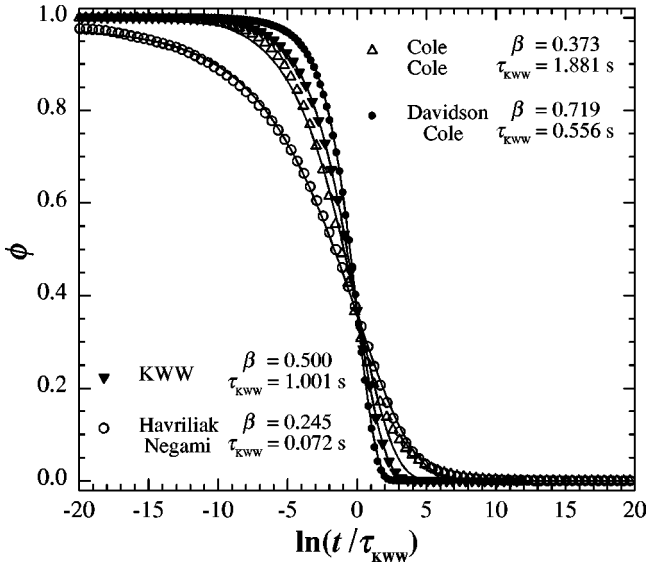

FIG. 5. Decay function calculated from Eq. (9) with the $G(\ln(\tau))$ obtained with SADSA for a Cole-Cole function ($\alpha=0.5$), Davidson-Cole function ($\gamma=0.5$), Havriliak-Negami function ($\alpha=0.6$, $\gamma=0.3$) and KWW function ($\beta=0.5$); —— Fitted curves to KWW functions, the resulting β and τ_{KWW} are indicated in the legend.

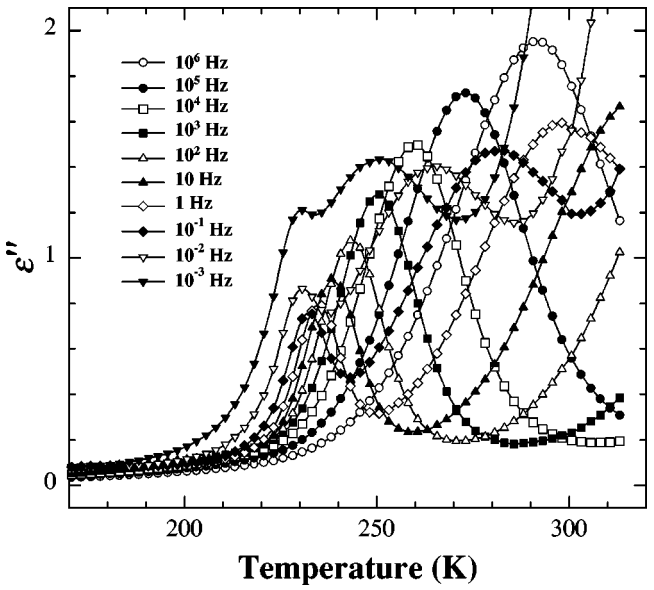

FIG. 6. $\varepsilon''(T)$ for α-PVDF, for frequencies $1\,\mathrm{mHz} \leqslant f \leqslant 1$ MHz. The lines are drawn to guide the eye.

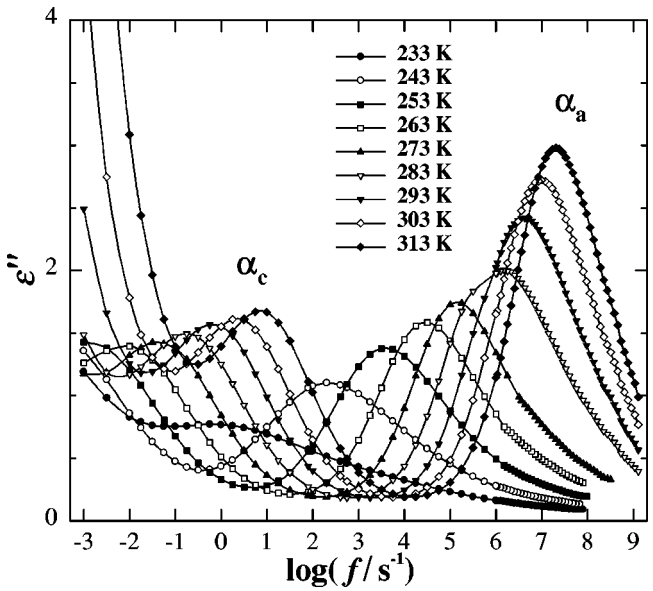

FIG. 7. $\varepsilon''(f)$ for α-PVDF, for temperatures 233 K $\leqslant T \leqslant$ 313 K. The lines are drawn to guide the eye.

The Havriliak-Negami decay function fit to a KWW gives $\beta = 0.245$, $\tau_{KWW} = 0.072$ s as compared to the shape parameters used in the simulation $\alpha = 0.6$, $\gamma = 0.3$, $\tau_0 = 1$ s, and quantitatively the sum of square residuals is higher than in the case of the Davidson-Cole function. A comparison can be made at this point among our results and those presented by Alvarez *et al.*[40] These authors sought the interconnection between Havriliak-Negami and KWW functions. They use the Imanishi *et al.*[12] algorithm to obtain among other things the three-dimensional and contour plots of the β values obtained for the different pairs of α and γ. Our results fit well in the corresponding contour.

Finally, for the KWW decay function the continuous curve represents the fitting to Eq. (1) and obviously gives an excellent agreement and a $\beta = 0.500$, $\tau_{KWW} = 1.001$ s, as expected, and a sum of least squares residuals three orders of magnitude less than above.

As a conclusion for this section on the results obtained with the SADSA procedure when extracting the distribution of relaxation times $G(\ln(\tau))$ from the computer-generated curves using the different empirical relaxation functions listed in Table I, we have checked that the program indeed finds a discrete distribution that follows very nearly the analytical distribution, which is known in those cases. Also the interconnection of the Havriliak-Negami decay function with a KWW stretched exponential is also demonstrated.

B. PVDF relaxation spectra

The relaxation spectra of α-PVDF as a function of temperature at different frequencies is shown in Fig. 6. At very low temperature a weak bump, not shown in the figure, arises from the local dipolar modes. The dielectric manifestation of the glass transition originated by cooperative dipolar motions in the amorphous phase, usually labeled as the β or the α_a relaxation, is the first intense peak that appears as the temperature increases. In this figure, it is clearly seen that the α_a mode shifts in temperature as the frequency increases; additionally, a broadening and enhancement of the peak intensity of the dielectric loss is observed. The presence of a relaxation labeled α_c on the high-temperature side of the α_a mode affects the intensity of this latter peak at very low frequencies ($f \leqslant 10^{-1}$ Hz). For frequencies below 10 Hz the α_c mode is observed and is more intense than the α_a mode. In Fig. 7 $\varepsilon''(f)$ is represented for 233 K $\leqslant T \leqslant$ 313 K for 1×10^{-3} Hz $\leqslant f \leqslant 1.8 \times 10^9$ Hz. The presence of the α_a and α_c modes is clearly seen in the frequency domain. Higher temperatures are not shown as the conductivity component becomes important and the results are too affected to be used in any of the precise analysis that are intended here. The SADSA procedure is then applied to the ten curves obtained with 5 K steps in the range 233 K $\leqslant T \leqslant$ 278 K and 10^{-3} Hz $\leqslant f \leqslant 1 \times 10^6$ Hz, where the α_a and α_c relaxations are complete and most suitable for analyzing it with the SADSA fitting procedure. The contribution of the dc conductivity was subtracted from the experimental data at low frequencies as a term whose expression is $\sigma = \sigma_0 / \epsilon_0 \omega$. The results of the fitting are shown as continuous curves in Fig. 8, the symbols being the experimental points. As usual, the fitted curve follows very closely the experimental results; the relaxation times distributions resulting from the best fit of the experimental results represented in Fig. 8 are shown in Fig. 9 for six of the ten temperatures chosen here. The results show clearly the existence of a bimodal distribution, a faster asymmetrical one, the segmental α_a relaxation, and the slower symmetric α_c mode. The distribution for the α_a mode becomes narrower as the temperature increases and its mean value shifts to lower τ's. The intensity of high τ extreme bins in each case is due to the edge effects inherent to numerical calculations when the tails of the curve are not completely defined, which is the case for the α_c mode at low temperatures as seen in Fig. 8. The results obtained for $G(\ln(\tau))$ from the dielectric loss curves are also used to simulate $\varepsilon'(\omega)$ according to Eq. (7) in the temperature range studied here, and the agreement with the experimental data is found to be excellent. Additionally, and for the first time for α-PVDF, with the knowledge of $G(\ln(\tau))$, the decay function

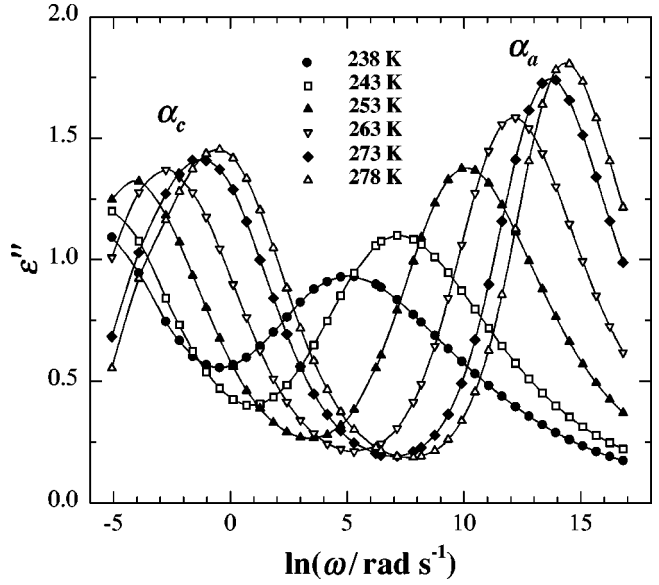

FIG. 8. $\varepsilon''(\omega)$ for α-PVDF, for temperatures 238 K $\leqslant T \leqslant$278 K. The symbols are the experimental points (without the dc conductivity), the continuous curves correspond to the results of the SADSA procedure.

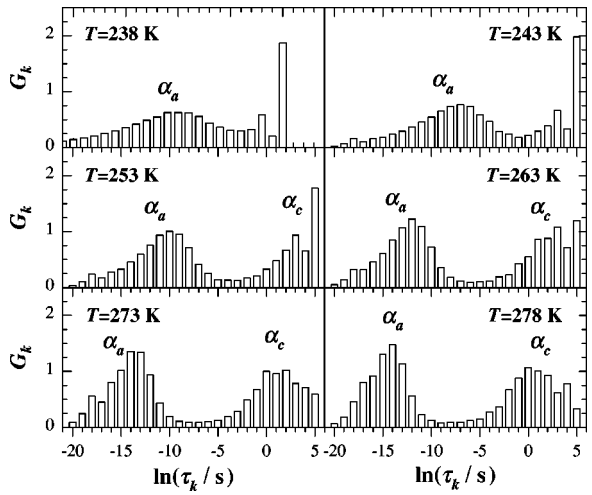

FIG. 9. G_k histograms extracted with the SADSA procedure from the $\varepsilon''(f)$ for α-PVDF, for temperatures 238 K $\leqslant T \leqslant$278 K.

$\phi(t)$ can be calculated at temperatures 233 K $\leqslant T \leqslant$278 K and the results are represented in Fig. 10. The existence of two relaxation processes is also clearly seen here and each decay curve has been fitted to a KWW stretched exponential with satisfactory results as can be seen in this latter figure from the good agreement among the symbols and the continuous curves, which result from the KWW fitting. In the inset of this figure the variation of the β parameter with temperature for the two different modes is plotted and shown to be significant for this material. A linear dependence in the temperature range explored here is found to be for both β_a and β_c KWW parameters:

$$\beta_a = -1.22 + 6.16 \times 10^{-3} T; \quad \beta_c = 1.46 - 4.08 \times 10^{-3} T, \quad 233 \text{ K} \leqslant T \leqslant 313 \text{ K}.$$

The increasing value found here for the β_a exponent as the temperature increases is explained as a consequence of

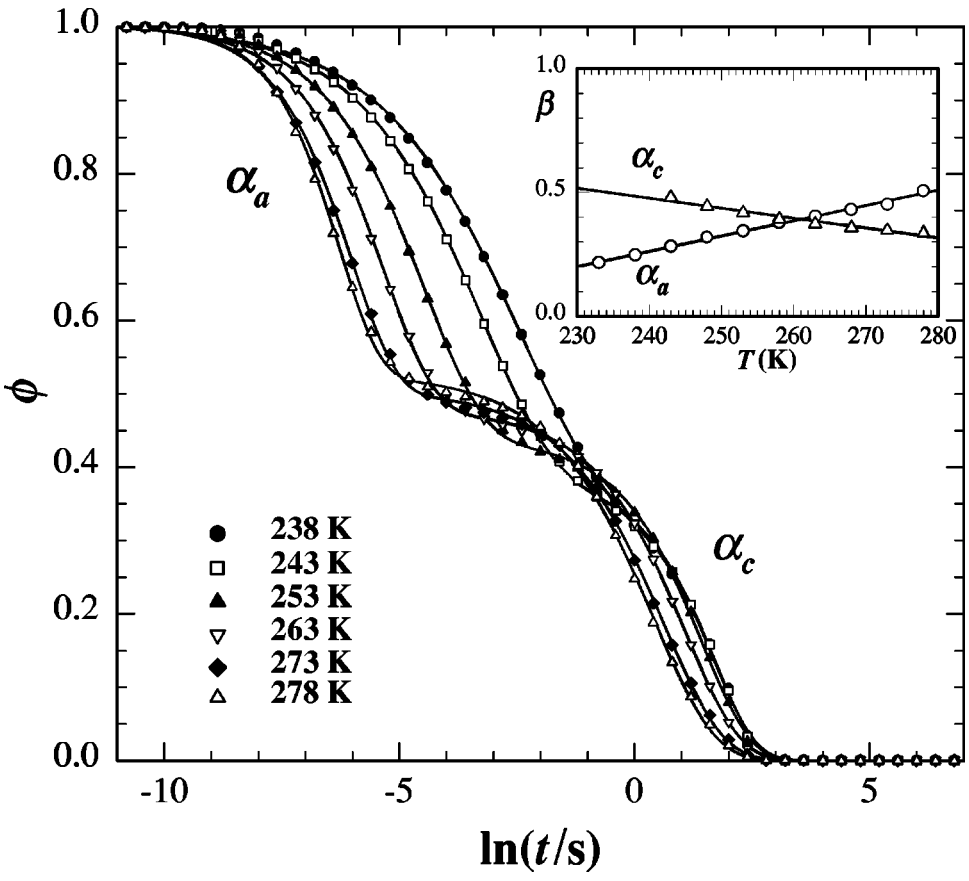

FIG. 10. Decay function for α-PVDF calculated from Eq. (9) with the $G_k(\ln(\tau_k))$ shown in Fig. 9 for temperatures 238 K $\leqslant T \leqslant$278 K. The continuous curves are the fittings to KWW decay functions. The inset shows the variation of the KWW β parameters with temperature.

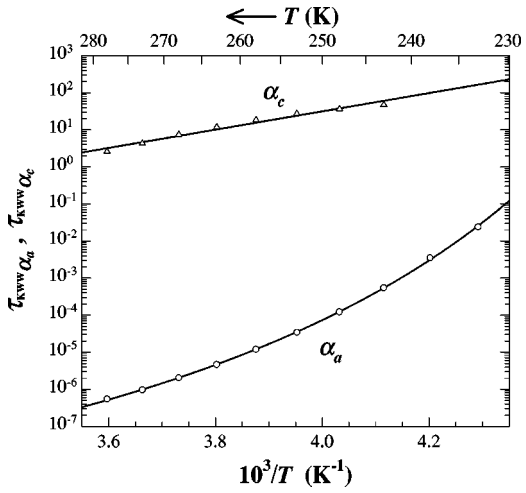

FIG. 11. Relaxation plots for α_a and α_c modes for α-PVDF, $\tau_{KWW}=f(10^3/T)$. The continuous curves are the fitting to VTF and Arrhenius expressions, respectively.

the reduction in size of the cooperative rearranging regions (CRR) introduced in the molecular kinetic theory proposed by Adam and Gibbs.[41] Ngai *et al.*[42] have proposed an extension of this model that takes into account the coupling between the CRR in a more complete theory for glass-forming liquids. They predict the behavior of the n parameter, which is related to β, $\beta=1-n$, to be dependent on the size, z^*, of the CRR and to increase with z^*. The increase of n as the temperature decreases is predicted. These authors apply their theory to low-molecular weight glass-forming liquids and find the expected behavior for *ortho*-terphenyl and 3-bromopenthane, while for glycerol there is no variation with decreasing temperature. The reported increase of β_a with temperature found here, is understood by considering that as the temperature increases the mode approaches a Debye behavior because the interaction between relaxing entities is not significant as the size of the CRR is reduced. The variation of n or β with temperature is to be related with the fragility of the material, which is measured in the relaxation plots $\tau(T)=f(1/T)$. The more fragile the material the more is its deviation from an Arrhenius dependence. From the fitting of the calculated $\phi(t)$ to 2 stretched exponentials, the KWW relaxation time is obtained in the temperature interval 233 K $\leqslant T \leqslant$ 313 K. The results of these calculations are shown on Fig. 11, where the curvature of the α_a plot is very apparent. The fit of these points (open circles) to a Vogel-Tammann-Fulcher (VTF) expression given in equation (4) results in the following parameters:

$$E_{VTF}=0.09 \text{ eV}, \quad T_0=185.2 \text{ K}, \quad \tau_{0_{VTF}}=5.2\times10^{-12} \text{ s}.$$

These VTF parameters agree very well to a previous determination made by us[18] by applying the SADSA to thermally stimulated depolarization curves and DS in a much more restricted frequency range. Also, these values compare well to those determined by Samara [22] at a pressure of 1 bar. Another consequence of the numbers obtained here by fitting the VTF relaxation plot is the calculation of the fragility parameter, m, as defined by Bohmer *et al.*[43]

$$m=\frac{E_{VTF}/kT_g}{(\ln 10)(1-T_0/T_g)^2}, \tag{13}$$

where m is an indication of the steepness of the variation of the material properties, i.e., viscosity, relaxation time, as T_g is reached. A high m value defines a very fragile material whereas a strong one will be characterized by small value for m. Bohmer *et al.*[43] compared different types of glass-forming materials, among them several amorphous polymers. The $m(T_g)$ values tabulated range from 46 (polyisobutylene) to 191 (polyvinylchloride). The $m(T_g)$ value calculated with the VTF parameters found in this work for α-PVDF is equal to 87, determined at the glass transition temperature taken as the temperature where the relaxation time is equal to 100 s. This fragility parameter indicates that PVDF is not a very fragile material as compared with the polymers reported by these authors. The value of the KWW parameter $\beta_a(T_g)$ is estimated to be 0.14, which does not agree with the general trend of the reported values in the cited work by Bohmer *et al.*[43] This low β value was to be expected due to the wide distribution found at low temperatures, which may be attributed to the existing strong chain interactions due to the electronegativity of the fluorine atoms. Also, the low fragility of α-PVDF can be associated to the semicrystalline nature of this polymer.

The same analysis is now made for the α_c mode and the results are shown for the variation of β_c on Fig. 10 and for the relaxation plot shown in Fig. 11. The parameter β_c is now a decreasing function of temperature and the relaxation plot shows an Arrhenius dependence for $\tau(T)$ with the following values for the pre-exponential and the energy factor:

$$\tau_0=4.3\times10^{-9} \text{ s}; \quad E=0.49 \text{ eV}.$$

This α_c mode is associated with molecular motions originated in the crystalline regions and it shifts very rapidly towards higher temperatures as the frequency increases. Nakagawa and Ishida[19] have explained the origin of this high-temperature relaxation as the result of molecular motions in the chain folds of the crystalline lamellas in addition to those in the interior of the crystals. These authors conclude that the folded chain is relatively mobile, while the motion of the chains inside the lamellas is restricted to rotations around the main chain axis. They found Arrhenius enthalpies in the range of 21 to 25 kcal/mole (0.89 to 1.08 eV), which are much higher than the values found here. Miyamoto *et al.*[20] interpreted the Arrhenius behavior for this relaxation as being originated by a two-site jump motion through the conformational change $TGT\bar{G}\leftrightarrow\bar{G}TGT$. They report a free Arrhenius energy of less than 1 kcal/mole and interpret the observed anisotropy of the α_c relaxation in α-PVDF as a change in conformation with internal rotation that can occur in the crystalline phase, with defects in the crystalline regions playing an important role in this mode.

Recently, sensitive NMR experiments[21] on α-PVDF have confirmed that the only molecular motion consistent with both dielectric and NMR measurements is the one initially proposed by Miyamoto *et al.*[20] The only discrepancy resides in the time scale of the motion, which is found to be in the NMR studies as equal to 20 ms at 370 K, while the previous dielectric studies place it in the range of 0.1 to 1 ms. Hirsch-

inger *et al.*[21] attributed these differences in time scale to the effect of chemical defects (head-head or tail-tail junctions) on the position of the loss maximum. If one calculates the relaxation time at 370 K from the Arrhenius parameters found in this work, one finds 20.3 ms in excellent agreement with the most recent studies. The agreement found here between NMR and DS discards the need to invoke the defects influence and simplifies the interpretation. Referring to the variation of the β_c parameter with temperature, the only determination of the variation with temperature of the parameters that characterize the distribution of relaxation times for a mode originated in the crystalline regions is, to the best of our knowledge, in lightly oxidized high-density polyethylene.[44] The author reports a linear dependence with temperature, with positive slope, for the Cole-Cole parameter. This is attributed to the presence of point defects, whose effect is expected to be significant due to their high population. In the sine-Gordon soliton model studied by this author the β_c value predicted for a polar polymer is 0.74 and independent of temperature, which does not correspond to our determination. These variations could be due to the conformational differences between α-PVDF and polyethylene already noted by the author who suggested that the model should be tested in zigzag planar polar polymers such as β-PVDF.

VI. CONCLUSIONS

We have presented an alternative method to extract from the dielectric relaxation function obtained by broad-band dielectric spectroscopy the distribution function of relaxation times. The advantages of our approach is that the profile of the distribution has not to be assumed *a priori*, the resulting quality of the fitting being much higher than by starting from analytical known expressions. In this way, hidden peaks can be detected and overlapping modes can be treated. The results with computer-generated curves whose distribution function is analytically known, give a discretized distribution of relaxation times, which follows extremely well the expected behavior for the symmetric Cole-Cole function as well as for the asymmetric Davidson-Cole, Havriliak-Negami, and KWW distribution functions.

When switching to the time domain, the decay functions are obtained from the knowledge of the distribution functions. These decay functions calculated from the computer-generated curves follow very closely a decay described by a stretched exponential provided that the distribution functions are asymmetric. The KWW β parameter can then be related to the α and γ parameters and the results found here agree very well with those of Alvarez *et al.*[40] reached by a quite different procedure. The SADSA method is a powerful technique to ensure that the fit is the best one and that a global minimum has been reached independently of the choice of the initial parameters set. The discretization of the distribution function avoids the use of Fourier transforms, without implying too long computing times. A typical fitting of $\varepsilon''(\omega)$ at one temperature with 37 points will consume typically 2 h in a Sun Ultra 1 work station. There are many problems where this technique can be applied as processes, which cannot be described by a single relaxation time and that are better understood if a summation of Debye contributions is assumed, are abundant in the literature.

The results of the analysis of the relaxation spectra of PVDF at different temperatures in a wide frequency range showed the presence of the α_a and α_c relaxation modes and the variation of the corresponding distribution of relaxation times with temperature was found. When switching to the time domain, the decay function was calculated following the procedure described above and fitted to two overlapping stretched exponentials. The observed variation of the β exponents with temperature for both modes explains why the master curves in a broad frequency range are not a good approximation as the shape parameters vary. The variation of the relaxation time with temperature, $\tau_{KWW}(T)$, follows a VTF dependence for the mode corresponding to the segmental motion in the amorphous phase of the material, while an Arrhenius dependence is found for the relaxation due to the conformational changes proposed in the pioneer dielectric work of Miyamoto *et al.*[20] and recently confirmed by Hirschinger *et al.*[21] by precise NMR experiments. The discrepancy in the estimated relaxation times at 370 K noted by the latter does not exist when estimated from our work where a wider frequency range and further numerical analysis are used.

ACKNOWLEDGMENT

We thank the Consejo Nacional de Investigaciones Científicas y Tecnológicas (CONICIT Proyecto G-97-000594) for their financial support.

[1] D. Boese and F. Kremer, Macromolecules **23**, 829 (1990).
[2] A. Schönhals, Macromolecules **26**, 1309 (1993).
[3] A. Schönhals and R. Stauga, J. Chem. Phys. **108**, 5130 (1998).
[4] K. S. Cole and R. H. Cole, J. Chem. Phys. **9**, 341 (1941).
[5] D. W. Davidson and R. H. Cole, J. Chem. Phys. **19**, 1484 (1951).
[6] S. Havriliak, Jr. and S. Negami, J. Polym. Sci., Part C: Polym. Symp. **14**, 99 (1966).
[7] F. Alvarez, A. Alegría, and J. Colmenero, Phys. Rev. B **44**, 7306 (1991).
[8] J. Colmenero, J. Non-Cryst. Solids **131-133**, 860 (1991).
[9] G. Williams and D. C. Watts, Trans. Faraday Soc. **66**, 80 (1970).
[10] K. L. Ngai, R. W. Rendell, A. K. Rajagopal, and S. Teitler, Ann. (N.Y.) Acad. Sci. **484**, 150 (1986).
[11] K. L. Ngai, R. W. Rendell, and A. F. Yee, Macromolecules **21**, 3396 (1988).
[12] Y. Imanishi, K. Adachi, and T. Kotaka, J. Chem. Phys. **89**, 7593 (1988).
[13] S. W. Provencher, Comput. Phys. Commun. **27**, 213 (1982).
[14] K. Karatasos, S. H. Anastasiadis, A. N. Semenov, G. Fytas, M. Pitsikalis, and N. Hadjichristidis, Macromolecules **27**, 3543 (1994).
[15] H. Schäfer, E. Sternin, R. Stannarius, M. Arndt, and F. Kremer, Phys. Rev. Lett. **76**, 2177 (1996).
[16] S. Kirkpatrick, C. D. Gelatt, Jr., and M. P. Vecchi, Science **220**, 671 (1983).

[17] M. Aldana, E. Laredo, A. Bello, and N. Suarez, J. Polym. Sci., Part B: Polym. Phys. **32**, 2197 (1994).
[18] M. Grimau, E. Laredo, A. Bello, and N. Suarez, J. Polym. Sci., Part B: Polym. Phys. **35**, 2483 (1997).
[19] K. Nakagawa and Y. Ishida, J. Polym. Sci., Polym. Phys. Ed. **11**, 1503 (1973).
[20] Y. Miyamoto, H. Miyaji, and K. Asai, J. Polym. Sci., Polym. Phys. Ed. **18**, 597 (1980).
[21] J. Hirschinger, D. Schaefer, H. Spiess, and A. Lovinger, Macromolecules **24**, 2428 (1991).
[22] G. Samara, J. Polym. Sci., Part B: Polym. Phys. **30**, 669 (1992).
[23] C. J. F. Böttcher and P. Bordewijk, *Theory of Electric Polarization*, Vol. II, 2nd. ed. (Elsevier, Amsterdam, 1978).
[24] S. Havriliak, Jr. and S. J. Havriliak, J. Polym. Sci., Part B: Polym. Phys. **35**, 1887 (1997).
[25] J. V. Bertelsen and A. Lindgård, J. Polym. Sci., Polym. Phys. Ed. **12**, 1707 (1974).
[26] A. Schönhals, Acta Polym. **42**, 149 (1991).
[27] A. D. Franklin and H. J. de Bruin, Phys. Status Solidi A **75**, 647 (1983).
[28] K. Liedermann and A. Loidl, J. Non-Cryst. Solids **155**, 26 (1993).
[29] J. Honerkamp and J. Weese, Continuum Mech. Thermodyn. **2**, 17 (1990).
[30] J. Weese, Comput. Phys. Commun. **69**, 99 (1992).
[31] P. Colonomos and R. G. Gordon, J. Chem. Phys. **71**, 1159 (1979).
[32] A. Bello, E. Laredo, and N. Suarez, *1995 IEEE Annual Report: Conference on Electrical Insulation and Dielectric Phenomena*, IEEE Publication No. 95CH35842, 1995, p. 440–443.
[33] W. H. Press, S. A. Teukosolsky, W. T. Vettering, and B. P. Flannery, *Numerical Recipes in Fortran, The Art of Scientific Computing*, 2nd. ed. (Cambridge University Press, Cambridge, 1992).
[34] N. Metropolis, A. Rosenbluth, M. Rosenbluth, A. Teller, and E. Teller, J. Chem. Phys. **21**, 1087 (1953).
[35] A. Corana, M. Marchesi, C. Martini, and S. Ridella, ACM Trans. Math. Softw. **13**, 262 (1987).
[36] H. Szu and R. Hartley, Phys. Lett. A **122**, 157 (1987).
[37] G. H. Weiss, M. Dishon, A. M. Long, J. T. Bendler, A. A. Jones, B. T. Inglefield, and A. Bandis, Polymer **35**, 1880 (1994).
[38] M. Dishon, J. T. Bendler, G. H. Weiss, J. Res. Natl. Inst. Stand. Technol. **95**, 433 (1990).
[39] C. P. Lindsey and E. D. Patterson, J. Chem. Phys. **73**, 3348 (1980).
[40] F. Alvarez, A. Alegría, and J. Colmenero, Phys. Rev. B **47**, 125 (1993).
[41] G. Adam and J. H. Gibbs, J. Chem. Phys. **43**, 139 (1965).
[42] K. L. Ngai, R. W. Rendell, and D. J. Plazek, J. Chem. Phys. **94**, 3018 (1991).
[43] R. Bohmer, K. L. Ngai, C. A. Angell, and D. J. Plazek, J. Chem. Phys. **99**, 4201 (1993).
[44] K. J. Wahlstrand, J. Chem. Phys. **82**, 5247 (1985).